Photosynth Res (2011) 108:61–76
DOI 10.1007/s11120-011-9654-0

REGULAR PAPER

A model for describing the light response of the nonphotochemical quenching of chlorophyll fluorescence

João Serôdio · Johann Lavaud

Received: 27 September 2010 / Accepted: 4 April 2011 / Published online: 23 April 2011

Abstract The operation of photosynthetic energy-dissipating processes is commonly characterized by measuring the light response of the nonphotochemical quenching (NPQ) of chlorophyll fluorescence, or NPQ versus E curves. This study proposes a mathematical model for the quantitative description of the generic NPQ versus E curve. The model is an adaptation of the Hill equation and is based on the close dependence of NPQ on the xanthophyll cycle (XC). The model was tested on NPQ versus E curves measured in the plant *Arabidopsis thaliana* and the diatom *Nitzschia palea*, representing the two main types of XC, the violaxanthin–antheraxanthin–zeaxanthin (VAZ) type and the diadinoxanthin–diatoxanthin (DD–DT) type, respectively. The model was also fitted to a large number of published light curves, covering the widest possible range of XC types, taxa, growth conditions, and experimental protocol of curve generation. The model provided a very good fit to experimental and published data, coping with the large variability in curve characteristics. The model was further used to quantitatively compare the light responses of NPQ and of PSII electron transport rate, ETR, through the use of indices combining parameters of the models describing the two types of light–response curves. Their application to experimental and published data showed a systematic large delay of the buildup of NPQ relatively to the saturation of photochemistry. It was found that when ETR reaches saturation, NPQ is on average still below one fifth of its maximum attainable level, which is only reached at irradiances about three times higher. It was also found that organisms having the DD–DT type of XC appeared to be able to start operating the XC at lower irradiances than those of the VAZ type.

Keyword index Chlorophyll fluorescence · Modelling · Nonphotochemical quenching · Photoacclimation · Photoprotection · Xanthophyll cycle

Notation

α	Initial slope of the ETR versus E curve
Ax	Antheraxanthin
DD	Diadinoxanthin
DT	Diatoxanthin
E	PAR irradiance (μmol m^{-2} s^{-1})
E_{50}	Irradiance level corresponding to 50% of NPQ_m in a NPQ versus E curve
E_k	Light-saturation parameter of the ETR versus E curve
ETR	PSII relative electron transport rate
ETR_m	Maximum ETR in a ETR versus E curve
F_o, F_m	Minimum and maximum fluorescence of a dark-adapted sample
F_s, F'_m	Steady state and maximum fluorescence of a light-adapted sample
NPQ	Nonphotochemical quenching
NPQ_m	Maximum NPQ value reached in a NPQ versus E curve
NPQ_{E_k}	Fraction of NPQ_m reached when $E = E_k$

J. Serôdio (✉)
Departamento de Biologia and CESAM—Centro de Estudos do Ambiente e do Mar, Universidade de Aveiro,
Campus de Santiago, 3810-193 Aveiro, Portugal
e-mail: jserodio@ua.pt

J. Lavaud
UMR CNRS 6250 "LIENSs," Institute for Coastal and Environmental Research (ILE), University of La Rochelle,
2 rue Olympe de Gouges, 17 000 La Rochelle, France

n	Sigmoidicity coefficient of the NPQ versus E curve
PSII	Photosystem II
RLC	Rapid light–response curve
VAZ	Vx–Ax–Zx XC
Vx	Violaxanthin
XC	Xanthophyll cycle
Zx	Zeaxanthin

Introduction

Photosynthesis requires a balance between maximizing light absorption and minimizing damages caused by excessively absorbed light energy. Under natural conditions, exposure to sunlight involves unavoidable risks to the photosynthetic apparatus because of the formation of reactive oxygen species of photosynthetic origin produced under excess light (Osmond et al. 1997; Ort 2001; Demmig-Adams and Adams 2006). The sustainment of prolonged photosynthetic activity under high solar irradiances is ensured by the regulation of the repartition of absorbed light energy between photochemistry and energy-dissipating pathways. The latter function as photoprotective process against permanent damages to the photosynthetic apparatus, or photoinhibition, and are therefore of considerable interest for understanding the resistance of photoautotrophs to environmental stress (Demmig-Adams and Adams 2006; Lavaud 2007; Li et al. 2009).

One of the most important photoprotective processes is the nonphotochemical quenching (NPQ). NPQ groups several pathways among which the thermal dissipation of excess energy (or q_E, the energy-dependent quenching, Müller et al., 2001) is considered as the most important. The q_E takes place in the light-harvesting antenna of the photosystem II (PSII). It relies on the presence of specific PSII antenna proteins (PsbS in plants, Li et al. 2000; LhcSR in green microalgae, Peers et al. 2009; and Lhcx in diatoms, Bailleul et al. 2010), the building of a transthylakoid proton gradient (ΔpH), and the subsequent enzyme-mediated operation (de-epoxidation) of the xanthophyll cycle (XC) (Goss and Jakob, 2010). The XC produces de-epoxidised forms of xanthophylls that are essential regulatory partners of q_E, especially in some groups of microalgae (such as the diatoms; Lavaud, 2007; Li et al. 2009; Goss and Jakob 2010). In plants, green algae and some Heterokontophyta (brown algae, Chrysophyceae), the XC is based on the reversible conversion of pigment violaxanthin (Vx) to the q_E-involved zeaxanthin (Zx), passing through the intermediate form antheraxanthin (Ax) (VAZ type of XC); in other algal groups, such as the diatoms, dinoflagellates, Xanthophyceae, and Haptophyta, the XC consists of the conversion between only two pigments, diadinoxanthin (DD) and the q_E-involved diatoxanthin (DT) (DD–DT type of cycle; Olaizola and Yamamoto 1994; Lavaud et al. 2004; Lavaud 2007). In phycobilisome-containing organisms, there is no XC (cyanobacteria) or its presence is uncertain (red algae) (Goss and Jakob 2010).

The operation of NPQ processes is usually quantified using variable chlorophyll fluorescence (Pulse Amplitude Modulation fluorometry, PAM), by calculating the fluorescence index NPQ, which is based on the relative difference between the maximum fluorescence measured in the dark-adapted state, F_m, and on exposure to light, F'_m (see Notation):

$$\mathrm{NPQ} = \frac{F_m - F'_m}{F'_m} \quad (1)$$

This index is a rearrangement of the Stern–Volmer equation and reflects the assumption that the reciprocal of fluorescence yield is proportional to the Zx or DT concentration (Bilger and Bjorkman 1990; Lavaud et al. 2002; Baker and Oxborough 2004). The NPQ index has been routinely used to quantify the operation of photoprotective processes as well as the extent of photoinhibitory damages. Under experimental conditions allowing to assume that the prevailing processes causing the quenching of fluorescence are of photoprotective nature, NPQ has been used as a measure of the overall photoprotective capacity of the photosynthetic apparatus (e.g., Dimier et al. 2007b; Lavaud et al. 2007).

One common way to characterize the operation of photoprotective processes or the susceptibility to photoinhibition is to quantify the light response of NPQ. This is done by constructing NPQ versus E curves that record the development of NPQ with increasing incident irradiance. These curves are analogous to the more frequently measured light–response curves of the PSII electron transport rate (ETR) in the sense that they represent the variation of steady-state photosynthetic activity between different light levels, thus not informing on the kinetics of NPQ generation, but on the NPQ attainable under each irradiance. The shape of NPQ versus E curve varies widely, regarding its both overall shape and the absolute NPQ values reached. Typically, NPQ increases monotonically with irradiance, varying from zero (measured in darkness) to maximum values that vary greatly with taxonomical groups, physiological state, environmental constraints, or light levels applied. The curve presents a variable degree of sigmoidicity, ranging from cases when NPQ starts to increase steeply from the lowest light levels, following a simple saturation-like pattern (no sigmoidicity), to cases when NPQ remains close to zero for a range of low-light levels, then showing an abrupt increase only for intermediate

irradiances before stabilizing at maximum values (highly sigmoid). Often, although the stabilization of NPQ is evident, a constant value is not reached within the range of irradiances applied and the maximum attainable NPQ cannot be estimated.

Light–response curves of NPQ have been analysed and interpreted on the basis of arbitrarily chosen features, by qualitatively describing its shape (e.g., low or high sigmoidicity) or by selecting NPQ values reached at particular E levels (e.g., NPQ at maximum applied E). The absence of an adequate descriptive model impedes the characterization of the curve along the whole range of irradiances applied. Also, the lack of a commonly used set of descriptive parameters makes it difficult to compare curves measured in different studies or experimental conditions or taxonomic groups.

This study proposes a simple mathematical model for the quantitative description of the generic NPQ versus E curve, by means of the estimation of a small number of physiologically meaningful parameters. The model is based on the close, but not absolute, dependence of NPQ on the operation of the XC through the light-induced de-epoxidation of PSII antenna pigments Vx or DD. To illustrate the main features and variability of the NPQ versus E curve, as well as the interpretation of model parameters, light–response curves were measured on a plant (*Arabidopsis thaliana* [L.]; VAZ type XC) and a diatom (*Nitzschia palea* [Kütz] W. Smith; DD–DT type XC) grown under experimental conditions expected to induce a large variability in curve shape and NPQ absolute values. The adequacy of the model was further tested by fitting it to published NPQ versus E curves measured on a large variety of photosynthetic organisms and experimental conditions and covering the widest possible range of NPQ values and curve shapes. The usefulness of the model was also illustrated by exploring the relationship between NPQ versus E curves and the photoacclimation status, characterized by light–response curves of the ETR.

Materials and methods

Model rationale

The model proposed to describe the light–response curve of NPQ is an adaptation of the Hill equation, originally derived in the context of ligand binding to macromolecules with multiple binding sites. This equation describes the variation of the number of filled binding sites with the increase in ligand concentration, and is routinely used to characterize the cooperativity of enzymatic reactions (Voet and Voet 1990). The use of the Hill equation for modelling the NPQ versus E curve is based on the main assumption that NPQ is mostly because of the operation of the XC coupled to the buildup of the transthylakoid ΔpH, or energy-dependent quenching (q_E; Müller et al. 2001), and that the other potential components of NPQ, the quenching because of state transitions (q_T) or to photoinhibition (q_I), are not expected to significantly affect the NPQ versus E curves (see Discussion). The analogy underlying this rationale is to consider the epoxidized XC pigments Vx and DD as representing the macromolecule of the Hill model and the transthylakoidal ΔpH-dependent protonation of specific light-harvesting complex (LHC) antenna sites as corresponding to the ligand concentration that bind to their multiple binding sites. At steady state, each irradiance level corresponds to a stable transthylakoidal ΔpH and resulting Vx or DD de-epoxidation and activation through protonation of LHC sites (the so-called "activation" of Zx and DT; Horton et al. 2000; Goss et al. 2006; Lavaud and Kroth 2006; Horton et al. 2008), and thus to a defined NPQ value. The NPQ versus E curve is thus proposed to be described by the equation:

$$\mathrm{NPQ}(E) = \mathrm{NPQ_m}\frac{E^n}{E_{50}^n + E^n}, \quad (2)$$

where $\mathrm{NPQ_m}$ is the maximum NPQ value reached during the light curve, E_{50} is the irradiance level for which NPQ attains 50% of $\mathrm{NPQ_m}$, and n is the Hill coefficient, characterizing the sigmoidicity of the curve. While the parameters E_{50} and n are directly adopted from the Hill equation (originally having only these two parameters), a third parameter, $\mathrm{NPQ_m}$, had to be considered to account for the variability in the absolute values of NPQ. Under the analogy with the ligand-binding context of the Hill equation, NPQ(E) is considered to represent the fraction of Vx or DD molecules de-epoxidized into Zx or DT and which have been "activated." As such, E_{50} represents the irradiance level necessary to de-epoxidize and "activate" 50% of convertible Vx or DD pool (ligand concentration resulting in half occupation of binding sites) necessary to reach the maximal NPQ level, $\mathrm{NPQ_m}$. Of potential importance for the characterization of the physiological processes underlying the NPQ versus E curve is the sigmoidicity parameter n, which measures the type and extent of the reaction cooperativity. In the case of $n < 1$, the curve displays a saturation-like increase asymptotically toward $\mathrm{NPQ_m}$, indicating the presence of a negatively cooperative reaction; if $n > 1$, the curve starts to present a sigmoidal shape, the sigmoidicity increasing with n, indicating a positively cooperative, or allosteric, reaction; and if $n = 1$, the model is reduced to the Michaelis–Menten equation, indicative of a noncooperative reaction.

Measurement of light–response curves

To test the adequacy of the model, Eq. 2 was first fit to NPQ versus E curves generated for organisms representative of the two types of XC, a plant (*A. thaliana*; VAZ type

of XC) and a diatom (*N. palea*; DD–DT type of XC), grown under light conditions expected to induce large variations in NPQ absolute values and in the shape of the NPQ light–response curve. Plants of *A. thaliana* (ecotype Columbia) were grown under controlled growth chamber conditions for 4–5 weeks under a 16:8 h light/dark cycle and 70% relative humidity. The light/dark temperatures were 22/20°C. Three irradiance levels were applied: 10 ("low light," LL), 75 ("moderate light," ML), and 150 μmol m^{-2} s^{-1} ("high light," HL). The diatom *Nitzschia palea* (Kütz.) W. Smith (collection of the Department of Biology, University of Aveiro) was grown photoautotrophically in unialgal semicontinuous batch 100-ml cultures in sterile natural seawater enriched with f/2 nutrients (Guillard and Ryther 1962). Cultures were grown at 20°C, under 20 (LL), 100 (ML), and 400 μmol photons m^{-2} s^{-1} (HL) in a 12:12 h light/dark cycle. Cells were harvested by centrifugation (3,000 × *g*, 10 min) during the exponential phase of growth and were resuspended in fresh growth medium supplemented with $NaHCO_3$ to a final concentration >10 μg Chl *a* ml^{-1}.

Light–response curves of NPQ and ETR were generated by exposing the samples to 7–12 levels of actinic light, up to 920 μmol m^{-2} s^{-1}. Samples were dark-adapted for 30 min before the start of the light curve to allow determination of fluorescence levels F_o (minimum fluorescence) and F_m, required for the calculation of NPQ (Eq. 1). Samples were light-activated before the start of each light–response curve, through exposure to low light of 54 μmol photons m^{-2} s^{-1} until a steady state in fluorescence was reached (minimum 15 min). Under each light level, a saturation pulse (0.8 s for *A. thaliana* and 0.6 s for *N. palea*) was applied and fluorescence levels F_s (steady-state fluorescence) and F'_m were recorded and used to calculate NPQ (Eq. 1) and ETR, using (Genty et al. 1989):

$$\mathrm{ETR} = E\frac{F'_m - F_s}{F'_m} \quad (3)$$

A different sample (plant leaf or algal culture aliquot) was used for measuring NPQ and ETR under each light level. Three replicated measurements were made for each light level. Light–response curves of ETR were described by fitting the model of Eilers and Peeters (1988) and by estimating the parameters α (the initial slope of the curve), ETR_m (maximum ETR), and E_k (the light-saturation parameter). The parameter E_k is commonly interpreted as a measure of the light level to which a sample is acclimated to, and commonly used to characterize its photoacclimation status (Behrenfeld et al. 2004).

Chlorophyll fluorescence yield was measured using a PAM fluorometer comprising a computer-operated PAM-Control Unit (Walz) and a WATER-EDF-Universal emitter–detector unit (Gademann Instruments GmbH, Germany), using a modulated blue light (LED-lamp peaking at 450 nm, half-bandwidth of 20 nm) as source for measuring, actinic, and saturating light (Cruz and Serôdio 2008). Fluorescence was measured using a 6-mm diameter Fluid Light Guide fiberoptics. In the case of *N. palea*, the fiberoptics was connected to a fluorescence cuvette (KS-101, Walz, Effeltrich, Germany).

Published light–response curves

The model was also fitted to published NPQ versus *E* curves, covering a wide range of taxonomic groups (higher plants, mosses, green algae, diatoms, dinoflagellates, etc.), XC types (VAZ, DD–DT, and absence of XC), mutants with variable degrees of impairment of the XC operation, habitats (land and aquatic higher plants; planktonic and benthic microalgae), growth conditions (e.g., low- and high-light), physiological state (heat stress or XC inhibitors), and fluorescence light–response curve measuring protocols (steady-state and rapid-light curves, RLCs). Only species with a known functional XC were considered. Studies presenting light curves having less than seven data points were not considered, because of the large errors in the model fitting and parameter estimation. For each study, when three or more light curves were available for each species and experimental treatment, only the two curves presenting the most extreme (higher and lower) NPQ values were used. Detailed information on the data used in the meta-analysis is summarised in Table 2. When available, the corresponding ETR versus *E* curves were also characterized by fitting the model of Eilers and Peeters (1988) and by estimating its parameters.

Some studies have reported the formation of NPQ in the dark (Perkins et al. 2010). This phenomenon was observed on diatoms (Jakob et al. 1999) and brown algae (Mouget and Tremblin 2002), and results in NPQ versus *E* curves showing a distinctive bi-phasic pattern, with NPQ decreasing from initial high values measured in the dark to a minimum under low-to-moderate-light levels (e.g., Geel et al. 1997; Serôdio et al. 2006). Being relevant only for a limited number of taxonomic groups and physiological conditions, this type of NPQ light–response curve was not considered in this study.

Model fitting and parameter estimation

The light–response curve models were fitted using a procedure written in Microsoft Visual Basic and based on Microsoft Excel Solver. Model parameters were estimated iteratively by minimizing a least-squares function, forward differencing, and the default quasi-Newton search method. The model can be easily fitted using commonly available

software packages. On preliminary tests, this method was compared with the fitting procedures implemented in Sigmaplot 9.0 (Systat Software, Inc., San Jose, USA) and Statistica 8.0 (Statsoft, Inc., Tulsa, USA) and no significant differences were found between the estimates of model parameters.

The standard errors of the parameter estimates were calculated following Ritchie (2008) and are asymptotic standard errors. For nonlinear models such as the one here tested, asymptotic standard errors may not be adequate, as they possibly underestimate the actual parameter uncertainty and cannot evaluate the eventual asymmetry of the confidence regions of estimated parameters (Johnson 2008). A number of alternative approaches exist, the best being based on Monte Carlo methods, such as the Boostrap (Press et al. 1996; Johnson 2008). However, the benefits of pursuing alternative methods, requiring substantially more computation time, depend on the magnitude of the uncertainty associated to parameter estimation. In this study, the use of asymptotic standard errors was justified by the finding that they were on average relatively low, in a majority of cases less than 10% of parameter estimates (see the following), in which case they can be considered acceptable (Tellinghuisen 2008).

Results

Model fitting to NPQ versus *E* curves

The light–response curves of NPQ measured in the plant *A. thaliana* and in the diatom *N. palea* acclimated to different growth light conditions showed a wide range of curve shapes, varying between two main types: (i) curves with low sigmoidicity, presenting a simple saturation-like pattern (e.g., Fig. 1a, HL), and (ii) curves with high sigmoidicity, presenting an initial period of low values, followed by a phase of rapid increase leading to a stage of plateau of maximum values (e.g., Fig. 2a, HL). In all cases, the model provided an excellent fitting to the experimental data throughout the whole range of light levels explaining always more than 99.1% of the data variability (Table 1). Although the residuals (Figs. 1b and 2b) showed in some cases a clearly nonrandom pattern of variation, values were typically low, between ±5%. The fitting of the model resulted in a large variation of model parameters with species and growth light conditions, following some consistent trends. For both *A. thaliana* and *N. palea*, the increase in growth light resulted in an increase in NPQ_m (Figs. 1a and 2a; Table 1). This increase in NPQ_m could be detected despite the fact that in most cases the curves did not reach their maximum values within the range of irradiances applied (e.g., Fig. 1a). Another effect of increasing growth light was the increase in the irradiance level for which the curves reached maximum values. For LL-grown samples, maximum NPQ was reached for lower irradiances, with the curves showing an overall lower sigmoidicity, whereas for HL-grown samples, curves reached saturation at much higher light levels. This trend could be well described by model parameter E_{50}, which increased with growth light in both species (Table 1).

The most noticeable difference between the NPQ light–response curves of *A. thaliana* and *N. palea* was the apparent curve sigmoidicity, with less sigmoid curves being found for the former and more sigmoid curves (and a larger variation) for the latter. This variation in curve sigmoidicity was well characterized by the model parameter *n*, which averaged 1.2 for *A. thaliana* (varying from 0.98 to 1.44), whreas reaching an average value of 2.11 for *N. palea* (varying from 1.61 to 2.61). However, a different pattern of variation was found for each species, with *n* decreasing with growth light in *A. thaliana* and increasing in *N. palea* (Table 1).

Model fitting to published NPQ versus *E* curves

The compilation of published light–response curves of NPQ allowed gathering a large number of datasets covering a wide range of NPQ absolute values and curve shapes. The model provided a very good fit to the published data, coping with the large diversity in curve characteristics resulting from different combinations of maximum NPQ values attained (NPQ_m), irradiance range of NPQ buildup (E_{50}), and curve sigmoidicity (*n*) (Table 2). Considering all cases, the model explained more than 96% of data variability, independently of type of XC (and XC-impaired mutants), species, growth conditions, and experimental protocol used for the generation of light curves. A summary of the meta-analysis carried out on the data set of published NPQ versus *E* curves is presented in Table 3. NPQ_m was the most variable parameter (coefficient of variation, c.v. = 112.5%), mostly responding to growth conditions, averaging 2.89 but reaching maximum values greater than 9 for diatoms and even higher for some mosses (Table 2). E_{50} ranged from 30–40 to greater than 3,500 μmol m^{-2} s^{-1}, in all cases attaining values well above growth irradiances (see the following). However, with few exception (the diatoms *Skeletonema costatum* and *Phaeocystis antarctica*, and the high-light-grown *A. thaliana*), all values of E_{50} greater than 1,200 μmol m^{-2} s^{-1} were obtained for *A. thaliana* mutants with impaired operation of the XC (Table 2). The *n* was the least variable parameter (c.v. = 50.8%), meaning that the curve shape remained relatively unaltered, and that the variability in the NPQ versus *E* curves was mainly because of changes in NPQ maximum values and in NPQ onset along the irradiance range. The *n* averaged 1.7, corresponding to a

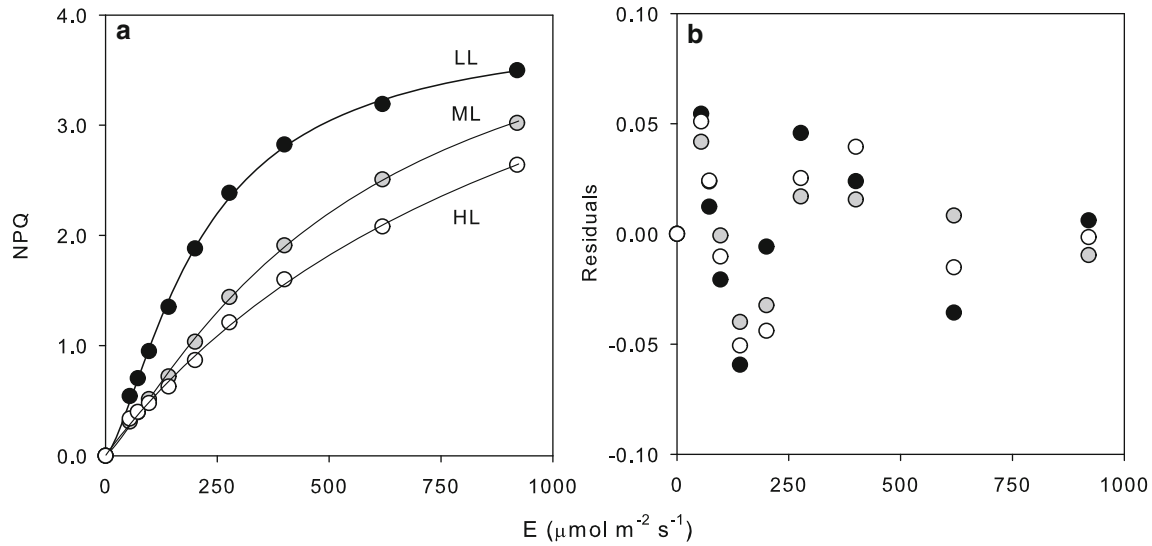

Fig. 1 Fitting of Eq. 2 to light–response curves of NPQ measured in the plant *A. thaliana* grown under low (LL), moderate (ML), and high light (HL). **a** Light–response curves (*data points*), fitted model (*lines*), and estimates of model parameters. **b** Residuals of the model fitting

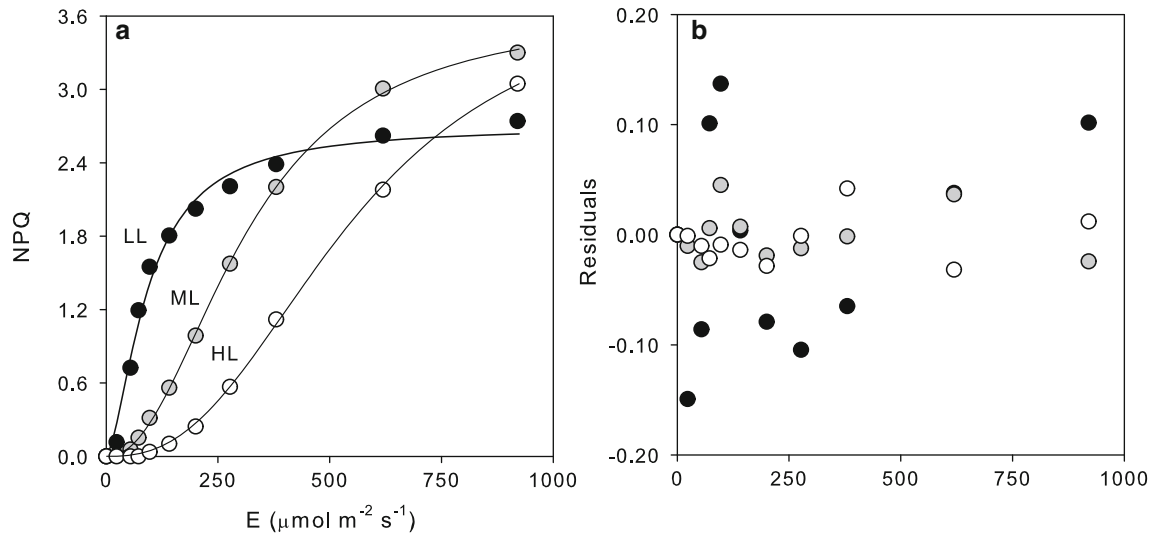

Fig. 2 Fitting of Eq. 2 to light–response curves of NPQ measured in the diatom *N. palea* grown under low (LL), moderate (ML), and high light (HL). **a** Light–response curves (*data points*), fitted model (*lines*), and estimates of model parameters. **b** Residuals of the model fitting

Table 1 Summary of the results of the fitting of the model to NPQ versus *E* curves measured in *A. thaliana* and *N. palea* grown under low (LL), moderate (ML), and high light (HL). Parameter estimates ± one standard error

		Model parameters			
		NPQ_m	E_{50}	n	r^2
A. thaliana	LL	3.91 ± 0.82	209.9 ± 8.31	1.44 ± 0.52	0.999
	ML	4.63 ± 0.24	542.0 ± 49.2	1.21 ± 0.04	0.999
	HL	5.90 ± 1.04	1141.0 ± 372.1	0.98 ± 0.06	0.998
N. palea	LL	2.70 ± 0.10	91.7 ± 7.01	1.61 ± 0.19	0.991
	ML	3.65 ± 0.05	312.6 ± 5.59	2.16 ± 0.05	0.999
	HL	3.86 ± 0.11	551.4 ± 15.8	2.55 ± 0.08	0.999

noticeable degree of sigmoidicity, although values around 1.0 (no sigmoidicity) or slightly lower (mostly mutants with impaired XC) as well as greater than 3.0 (very high sigmoidicity) were also found (Table 2).

When comparing different XC types, no clear differences were found between model parameters, because of the large overlap of their range of variation. Model parameters appeared to depend mostly on growth conditions, as larger variations could be found within the same species than among different taxonomic groups. The model also described very well the light–response curves of NPQ for composite samples (phytoplankton and microphytobenthos). Model parameters varied independently from

each other, as no significant correlations were found between NPQ_m, E_{50}, and n, either when considering all data pooled together or when considering for separate for each XC type.

Despite the low number of data points forming most NPQ versus E curves, standard errors of parameter estimates were on average relatively low (15.6, 27.3, and 12.2% of estimates for NPQ_m, E_{50}, and n, respectively). However, standard errors were typically much higher in the cases when XC was impaired (24.5, 43.9, and 13.5% for NPQ_m, E_{50}, and n, respectively), indicating that a high level of precision in the estimation of model parameters can be expected for samples under natural conditions. For the data used for comparing VAZ and DD–DT organisms, in a majority of cases (78.8, 70.0, and 60.6% for NPQ_m, E_{50}, and n, respectively), standard errors remained less than 10% of parameter estimates.

Considering the published data, the effects of growth light levels on model parameters were identical to those described for the experimental data of this study. When compared with lower-light conditions, NPQ light–response curves of samples acclimated to high-light showed higher values of NPQ_m (Bilger and Bjorkman 1990; Burritt and MacKenzie 2003; Müller et al. 2004; Ralph and Gademann 2005; Rodríguez-Calcerrada et al. 2007; Cruz and Serôdio 2008) and, with the exception of Ralph and Gademann (2005), all these studies showed a similar increase in E_{50} with growth light. The model also fitted very well with the light–response curves of NPQ with impaired functioning of the XC, illustrating the usefulness of estimating model parameters to characterize quantitatively the effects on NPQ of inhibitors (e.g., Bilger and Bjorkman 1990), mutations (e.g., Niyogi et al. 1998), or changes in temperature (Ralph et al. 2001).

Finally, the model was also found to be adequate to describe NPQ versus E curves generated under nonsteady-state conditions, i.e., derived from RLCs. The comparison of the model parameters estimated for light curves of different light steps showed the same pattern on VAZ and DD–DT samples, with shorter light steps resulting in lower NPQ_m and higher E_{50}, wheras n not showing any consistent trend (Ralph and Gademann 2005; Perkins et al. 2006).

Relationship between NPQ and ETR light–response curves

To illustrate the application of the model to evaluate to what extent the NPQ response to light is related to the photoacclimation status, the light levels required for induction of NPQ and for photochemistry or ETR saturation were compared. A simple form of achieving this is by the direct comparison of model parameters E_{50} and E_k estimated for the two types of light–response curves. These parameters have the advantage of being measured in the same scale (PAR irradiance, μmol m^{-2} s^{-1}) and of being independent of the units used to measure photosynthetic rates, ETR or NPQ, which can vary with the method in use (the case of photosynthesis) or instrument settings (the case of ETR).

For the experimental data obtained in this study, the increase in growth irradiance induced a substantial change in the photoacclimation status, noticeable by a clear change in the ETR versus E curves. As a result, the increase observed for E_{50} was followed by a similarly large increase in E_k, because of the decrease of α and the increase of ETR_m, both in *A. thaliana* (Fig. 3) and in *N. palea* (Fig. 4). However, E_{50} was found to be in all cases higher than E_k, by 3.7 and 2.5 times, on average, for *A. thaliana* and *N. palea*, respectively (2.90 for the whole data). This result indicates that the light-induced buildup of substantial values of NPQ started only after linear electron transport reached near saturation. Furthermore, it shows that a large fraction of E_{50} variability was related to variations in the photoacclimation status because of different growth light conditions, as E_{50} increased linearly with E_k, for both the plant and the diatom (although the correlation was not statistically significant, but a clear linear trend is obvious; Fig. 5). This analysis also showed that the slope of the regression line of E_{50} on E_k was higher for *A. thaliana* than for *N. palea*, indicating that, for the same photoacclimation status (the same E_k), the plant requires a higher light level for NPQ to reach 50% of its maximum capacity. Or, in other words, that NPQ is induced latter in the range of irradiances in the plant than in the diatom.

Interestingly, the analysis of the subset of published data presenting both NPQ and ETR light–response curves showed the same generic trend. When pooling together the published and experimental data for samples with fully operational XC (i.e., excluding mutants or samples treated with XC inhibitors) and E_k estimates only based on steady-state light curves (i.e., excluding RLCs as E_k estimation is largely dependent on light step duration; Serôdio et al. 2006), the ratio E_{50}/E_k was found to be higher on organisms having a VAZ type of XC and to differ significantly from those having a DD–DT type (3.32 and 2.39, respectively; t-test $P = 0.038$; Fig. 6a).

Another way to compare the light responses of NPQ and ETR is to calculate the fraction of NPQ that is formed when ETR approaches saturation (i.e., when $E = E_k$), or:

$$NPQ_{E_k} = \frac{NPQ(E_k)}{NPQ_m} \quad (4)$$

Low values of NPQ_{E_k} indicate that when photochemistry saturates, NPQ is still not significantly developed (corresponding to high E_{50}/E_k), whereas high values indicate that NPQ responds more promptly to light increase and the approach of ETR saturation

Table 2 Results of fitting of Eq. 2 to published NPQ versus E curves. Parameter estimates ± one standard error

XC type	Taxon		LC	Treatment	Model parameters			r^2	Reference
					NPQ_m	E_{50}	n		
VAZ	Magnoliophyta (flowering plants)	*Arabidopsis thaliana*	SS	wt 10°C	2.07 ± 0.04	113.6 ± 6.0	1.11 ± 0.08	0.998	Havaux and Kloppstech (2001)
				wt 25°C	2.98 ± 0.40	1,118.0 ± 293.8	1.09 ± 0.11	0.996	
				npq1 10°C	1.68 ± 0.25	636.5 ± 587.0	0.40 ± 0.06	0.998	
				npq1 25°C	1.16 ± 0.22	867.1 ± 557.5	0.63 ± 0.10	0.995	
			SS	Li-1	3.76 ± 0.18	563.8 ± 40.6	1.83 ± 0.16	0.998	Jung and Niyogi (2009)
				Sf-2	4.12 ± 0.16	661.9 ± 33.7	2.03 ± 0.13	0.999	
				Col-0	3.29 ± 0.19	683.7 ± 55.0	1.84 ± 0.16	0.998	
				Ws-2	3.32 ± 0.19	599.8 ± 49.1	1.96 ± 0.21	0.997	
			SS	wt	2.06 ± 0.08	184.1 ± 13.4	2.21 ± 0.32	0.993	Lokstein et al. (2002)
				lut1	1.52 ± 0.06	195.5 ± 13.7	2.28 ± 0.33	0.994	
				lut2	1.76 ± 0.10	231.0 ± 22.2	1.72 ± 0.22	0.995	
				aba1	2.36 ± 0.19	251.1 ± 43.2	1.14 ± 0.13	0.996	
				lut2aba1	1.17 ± 0.07	214.7 ± 30.6	1.08 ± 0.10	0.997	
			SS	wt	3.22 ± 0.22	822.2 ± 90.9	1.46 ± 0.15	0.993	Müller-Moulé et al. (2002)
				vtc2	3.86 ± 0.22	1,606.8 ± 137.5	1.32 ± 0.05	0.957	
			SS	wt LL	2.99 ± 0.22	993.6 ± 96.6	1.95 ± 0.21	0.998	Müller-Moulé et al. (2004)
				vtc2 LL	4.52 ± 1.08	2,492.1 ± 700.8	1.49 ± 0.15	0.999	
				vtc2npq4 LL	2.03 ± 0.32	2,556.4 ± 402.8	1.73 ± 0.08	0.991	
				vtc2npq1 LL	2.51 ± 1.41	2,597.0 ± 1,777.5	1.43 ± 0.26	0.998	
				wt HL	4.55 ± 6.55	4,082.0 ± 5,997.8	1.47 ± 0.37	0.998	
				vtc2 HL	6.82 ± 2.35	4,133.0 ± 1,851.3	1.24 ± 0.10	0.999	
				vtc2npq4 HL	1.82 ± 1.00	3,527.3 ± 2,314.0	1.39 ± 0.21	0.996	
				vtc2npq1 HL	1.80 ± 1.84	3,502.8 ± 4,087.1	1.39 ± 0.32	0.996	
			SS	wt	2.21 ± 0.10	457.0 ± 26.5	1.48 ± 0.16	0.993	Munekage et al. (2002)
				pgr5	1.77 ± 3.20	1,478.1 ± 5,634.7	0.81 ± 0.45	0.957	
			SS	wt	2.25 ± 0.11	503.2 ± 39.4	1.44 ± 0.07	0.999	Munshi et al. (2006)
				crr6	2.00 ± 0.07	397.7 ± 22.5	1.60 ± 0.08	0.999	
				crr6CRR6	2.01 ± 0.08	365.2 ± 24.2	1.65 ± 0.11	0.999	
			SS	wt	4.47 ± 1.24	1,894.4 ± 746.9	1.34 ± 0.17	0.995	Niyogi et al. (1998)
				npq1	1.92 ± 0.81	1,877.4 ± 1,686.5	0.90 ± 0.18	0.988	
				npq2	3.23 ± 0.35	1,156.2 ± 207.4	1.32 ± 0.11	0.997	
		Begonia × *erythrophylla*	SS	LL	1.27 ± 0.04	388.3 ± 14.1	3.51 ± 0.36	0.992	Burritt and Mackenzie (2003)
				LL/HL	1.77 ± 0.05	467.3 ± 15.8	2.95 ± 0.23	0.997	
				HL	2.83 ± 0.17	618.3 ± 38.6	2.82 ± 0.32	0.995	

Table 2 continued

XC type	Taxon		LC	Treatment	Model parameters			r^2	Reference
					NPQ_m	E_{50}	n		
		Hedera canariensis	SS	LL	3.61 ± 0.04	382.6 ± 6.3	2.90 ± 0.13	0.999	Bilger and Bjorkman (1990)
				LL + DTT	1.14 ± 0.18	656.2 ± 218.9	1.09 ± 0.20	0.987	
				HL	5.34 ± 0.33	761.1 ± 59.6	2.05 ± 0.24	0.996	
				HL + DTT	1.48 ± 0.05	437.0 ± 27.8	2.20 ± 0.26	0.994	
		Quercus petraea	SS	Dense	2.23 ± 0.03	158.2 ± 6.35	1.83 ± 0.13	0.998	Rodríguez-Calcerrada et al. (2007)
				Edge	5.55 ± 0.11	423.2 ± 13.3	2.04 ± 0.10	0.999	
		Zostera marina	SS	LL	0.87 ± 0.15	797.3 ± 302.0	1.01 ± 0.14	0.995	Ralph and Gademann (2005)
			SS	HL	3.12 ± 0.25	400.5 ± 65.3	1.30 ± 0.16	0.995	
			RLC5	HL	1.36 ± 0.06	276.9 ± 26.9	1.39 ± 0.17	0.997	
			RLC10	HL	2.34 ± 0.17	399.0 ± 60.7	1.02 ± 0.11	0.997	
			RLC40	HL	3.37 ± 0.15	360.7 ± 30.4	1.45 ± 0.12	0.998	
	Bryophyta (mosses)	*Eurhynchium crassinervium*	SS		5.79 ± 0.58	237.9 ± 34.7	1.53 ± 0.12	0.998	Marschall and Proctor (2004)
		Pogonatum urnigerum			5.45 ± 0.48	584.7 ± 65.2	1.79 ± 0.15	0.998	
		Polytrichum juniperinum			5.90 ± 0.34	689.3 ± 34.3	2.68 ± 0.17	0.998	
		Tortula (Syntrichia) ruralis			12.23 ± 0.42	458.6 ± 16.5	2.61 ± 0.15	0.999	
		Racomitrium aquaticum			26.27 ± 3.23	830.8 ± 92.8	2.33 ± 0.18	0.999	
		Trichocolea tomentella			1.45 ± 0.06	68.7 ± 4.5	2.36 ± 0.33	0.992	
	Chlorophyta (green algae)	*Chara corallina*	SS		1.67 ± 0.04	34.0 ± 0.5	6.80 ± 0.73	0.993	Krupenina and Bulychev (2007)
		Chlamydomonas reinhardtii	SS	wt	1.83 ± 1.46	1,010.0 ± 1,660.0	0.81 ± 0.15	0.992	Elrad et al. (2002)
				npq5	0.19 ± 0.01	56.2 ± 3.58	3.66 ± 0.74	0.986	
		Picochlorum sp.	SS		1.88 ± 0.29	410.2 ± 142.0	1.06 ± 0.20	0.975	Dimier et al. (2007a)
	Eustigmatophyceae	*Nannochloropsis oculata*	RLC10		1.01 ± 0.06	224.5 ± 31.7	1.01 ± 0.08	0.998	Cosgrove and Borowitzka (2006)
DD-DT	Bacillariophycea (diatoms)	*Chaetoceros socialis*	SS		5.71 ± 0.08	149.4 ± 4.8	1.88 ± 0.10	0.999	Dimier et al. (2007b)
		Skeletonema marinoi			1.27 ± 0.03	233.0 ± 9.3	1.95 ± 0.13	0.998	
		Thalassiosira rotula			1.14 ± 0.18	198.9 ± 89.8	0.89 ± 0.23	0.977	
		Fragilariopsis cylindrus	SS	5 μmol m^{-2} s^{-1}	1.00 ± 0.18	637.5 ± 266.1	1.08 ± 0.23	0.966	Kropuenske et al. (2009)
				65 μmol m^{-2} s^{-1}	0.74 ± 0.08	1,023.1 ± 233.6	1.05 ± 0.9	0.996	
				125 μmol m^{-2} s^{-1}	0.59 ± 0.12	1,024.5 ± 540.6	0.94 ± 0.13	0.986	
		Phaeodactylum tricornutum	SS		2.30 ± 0.10	367.6 ± 24.1	2.59 ± 0.45	0.984	Lavaud et al. (2007)
		Skeletonema costatum			2.77 ± 0.75	2,825.9 ± 1,569.0	0.86 ± 0.08	0.998	
		Thalassiosira oceanica			0.88 ± 0.13	859.4 ± 282.2	0.95 ± 0.13	0.992	
		Thalassiosira pseudonana			1.05 ± 0.04	276.8 ± 18.4	1.96 ± 0.22	0.993	

Table 2 continued

XC type	Taxon		LC	Treatment	Model parameters			r^2	Reference
					NPQ_m	E_{50}	n		
		Thalassiosira weissflogii			1.58 ± 0.03	227.1 ± 8.3	2.70 ± 0.22	0.996	
		Phaeodactylum tricornutum	SS	IL	9.30 ± 0.10	288.5 ± 6.2	2.77 ± 0.16	0.999	Lavaud et al. (2002)
				CL	2.16 ± 0.08	334.4 ± 17.2	3.22 ± 0.71	0.980	
		Navicula phyllepta	RLC10		0.19 ± 0.06	1,057.6 ± 731.3	1.01 ± 0.36	0.976	Perkins et al. (2006)
			RLC30		0.54 ± 0.07	972.2 ± 370.1	0.73 ± 0.11	0.997	
			RLC60		0.91 ± 54.5	450.0 ± 54.5	1.55 ± 0.28	0.990	
			SS		2.90 ± 0.57	1,152.8 ± 463.0	1.10 ± 0.26	0.989	
		Nitzschia palea	SS	LL	3.48 ± 0.17	115.8 ± 12.2	1.38 ± 0.15	0.991	Cruz and Serôdio (2008)
				HL	5.62 ± 0.24	399.9 ± 27.1	1.58 ± 0.08	0.999	
	Dinophyta (dinoflagellates)	*Symbiodinium* sp.	RLC5	25°C	0.15 ± 0.01	143.3 ± 10.5	2.39 ± 0.32	0.996	Ralph et al. (2001)
				33°C	0.53 ± 0.05	115.8 ± 22.5	1.21 ± 22.5	0.994	
				37°C	1.20 ± 0.05	77.3 ± 6.7	1.18 ± 0.08	0.998	
				38°C	0.37 ± 0.01	39.9 ± 2.2	1.66 ± 0.17	0.995	
	Haptophyta	*Phaeocystis antarctica*	SS	5 μmol m^{-2} s^{-1}	0.27 ± 0.03	426.7 ± 49.7	1.93 ± 0.29	0.990	Kropuenske et al. (2009)
				65 μmol m^{-2} s^{-1}	1.49 ± 1.01	2,953.0 ± 3,309.0	1.07 ± 0.27	0.985	
				125 μmol m^{-2} s^{-1}	0.84 ± 0.13	755.1 ± 175.0	1.94 ± 0.56	0.986	
Composite		Microphytobenthos	RLC50		4.09 ± 0.12	349.2 ± 17.8	2.39 ± 0.26	0.994	Herlory et al. (2007)
			N-SLC		3.72 ± 0.13	546.2 ± 35.5	1.49 ± 0.10	0.996	
		Phytoplankton	SS	No mixing	5.07 ± 0.52	546.6 ± 85.5	1.42 ± 0.13	0.998	Kromkamp et al. (2008)
				Mixing	1.85 ± 0.09	446.4 ± 21.9	2.73 ± 0.24	0.997	

Composite samples containing organisms with different XC types; *LC* light curve protocol; *SS* steady state; *LL* low light; *RLCx* rapid light curve *x* seconds light step; *N-SLC* nonsequential light curve; *Treatment* conditions applied before the measurement of the light curves (PAR, temperature); growth conditions when more than one curve available for the same taxon—*HL* high light; *DTT* XC inhibitor dithiothreitol; *LL/HL* transfer from LL to HL; *Dense* plants from dense forest stand; *Edge* plants from forest edge; *IL* intermittent light; *CL* continuous light; *wt* wild type; *aba1*, *crr6*, *CRR6*, *lut1*, *lut2*, *lut2*, *npq1*, *npq2*, *npq4*, *npq5*, *vtc2* mutants; *LI-1*, *Sf-2*, *Col-0*, *Ws-2 Arabidopsis* accessions; *Mixing* water column mixing

Table 3 Summary of the meta-analysis of the results of the fitting of the model to published NPQ versus *E* curves (listed in Table 2). Mean values ± one standard error

XC type	Model parameters		
	NPQ_m	E_{50}	n
VAZ	3.30 ± 0.49	926.7 ± 135.1	1.77 ± 0.13
DD–DT	1.88 ± 0.41	657.9 ± 145.9	1.60 ± 0.14
Mixed	3.68 ± 0.67	472.1 ± 47.3	2.01 ± 0.33
All	2.89 ± 0.35	824.3 ± 99.2	1.73 ± 0.09

(corresponding to low E_{50}/E_k). Considering both published and experimental data (the data subset used early for comparing E_{50}/E_k), NPQ_{E_k} averaged 0.16, and remained less than 0.35, indicating that when $E = E_k$, NPQ hardly reached over one third of the maximum attainable level. Confirming the expected inverted relationship between NPQ_{E_k} and E_{50}/E_k, significantly lower values were found for organisms with a VAZ type of XC than for those with the DD–DT type (0.14 and 0.21, respectively; *t*-test, $P = 0.023$; Fig. 6b).

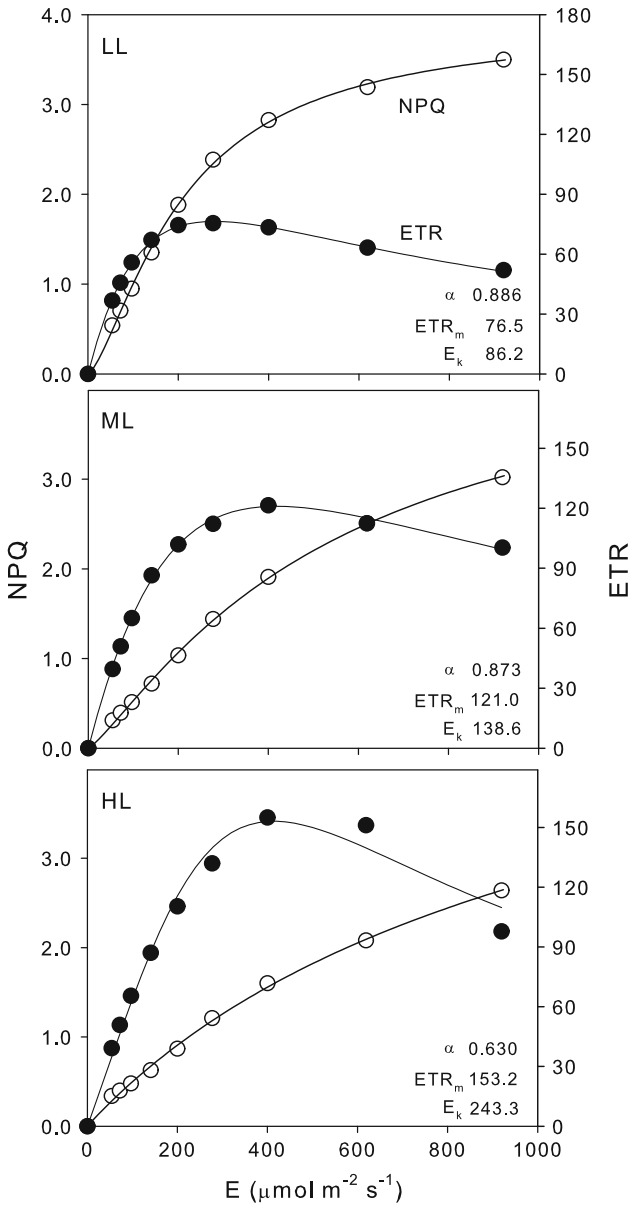

Fig. 3 Comparison between the light–response curves of NPQ and of ETR of *A. thaliana* grown under low (LL), moderate (ML), and high light (HL). Estimates of the parameters of the model of Eilers and Peeters (1988) fitted to the ETR versus *E* curves are presented. Estimates of the parameters of the curves fitted to the NPQ versus *E* curves are presented in Table 2

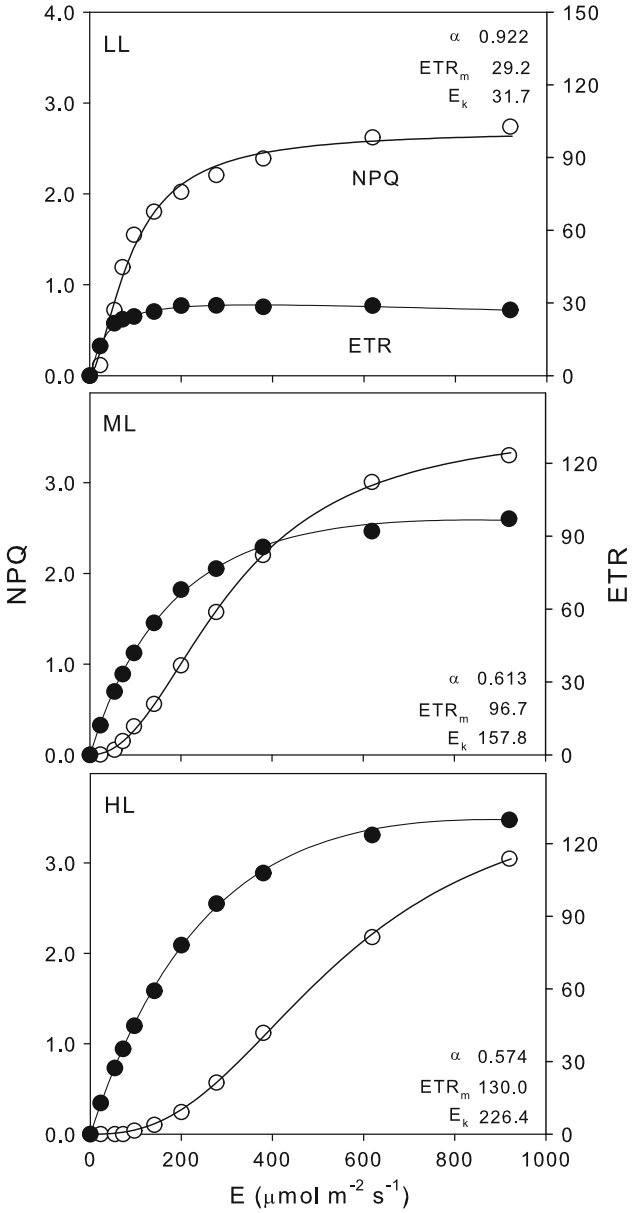

Fig. 4 Comparison between the light–response curves of NPQ and ETR of *N. palea* grown under low (LL), moderate (ML), and high light (HL). Estimates of the parameters of the model of Eilers and Peeters (1988) fitted to the ETR versus *E* curves are presented. Estimates of the parameters of the curves fitted to the NPQ versus *E* curves are presented in Table 2

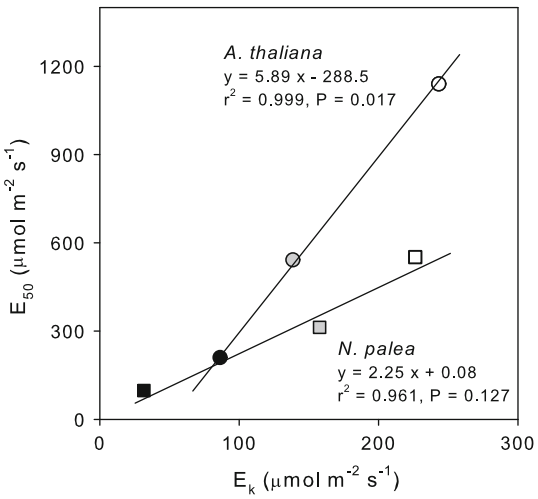

Fig. 5 Relationship between the parameter E_{50} of Eq. 2 fitted to the NPQ versus E curves and the parameter E_k of the Eilers and Peeters (1988) model fitted to the ETR versus E curves, for the plant *A. thaliana* (*circles*) and the diatom *N. palea* (*squares*) grown under high (*white*), moderate (*gray*), and low light (*black*)

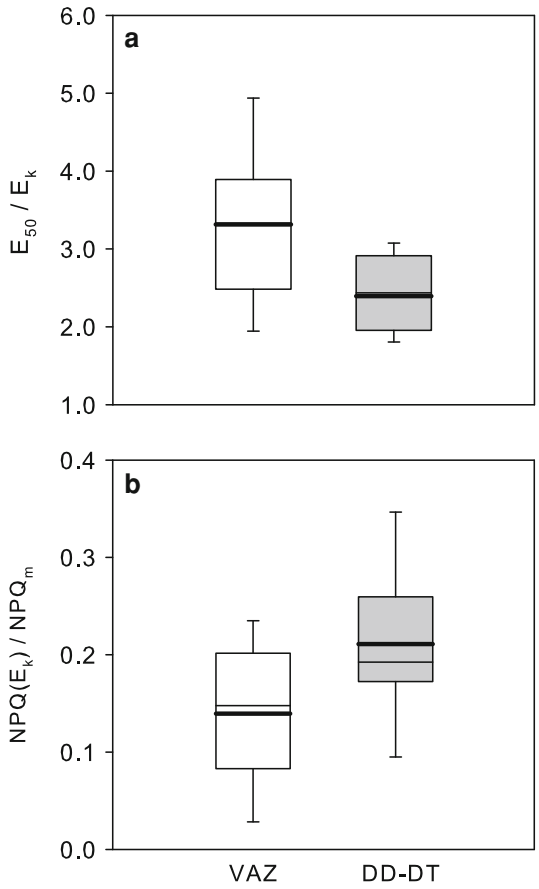

Fig. 6 Comparison between the ratios E_{50}/E_k (**a**) and NPQ(E_k)/NPQ_m (**b**) as calculated for the published (excluding cases with impaired XC operation) and experimental (this study) light–response curves of NPQ and ETR in VAZ and DD–DT types of XC. *Bars* represent one standard error, *boxes* represent the lower (25%) and upper (75%) quartiles, and the *thin* and *thick* horizontal lines inside the boxes represent the mean and the median, respectively

Model fitting and parameter estimation

Despite the usually reduced number of data points in the analyzed NPQ light–response curves (average 9.7, maximum 13), the model proposed in this study was found to be easily fitted to experimental curves, in most cases yielding parameter estimates virtually independently from the start values used in the iterative fitting procedure (although realistic start values allows a more rapid and precise parameter estimation). The main problem found when trying to fit Eq. 2 to NPQ versus E curves occurred when the curves were very close to linear, showing no clear features, such as sigmoidicity or saturation. This resulted in that a similarly good fit could be reached with different combinations of model parameters values. Still, this occurred only in relatively small number of cases, such as the case of the diatom *Skeletonema costatum* (Lavaud et al. 2007) and some *A. thaliana* mutants with severe impairment of XC operation, for which some degree of uncertainty remain associated to the presented parameter estimates.

This problem seems to result from the common situation of having light–response curves constructed with the main purpose of characterizing the ETR versus E curves, NPQ having only a secondary interest. As it often happens that the NPQ approaches its maximum for light levels much above the range used for measuring ETR, the NPQ versus E curve may result truncated and its complete shape may not be available for model fitting. Yet the relationship established between NPQ and ETR light curves in similar data may be used to impose boundaries to the model parameter estimates, and thus help to reach a single set of meaningful values.

Discussion

Model assumptions

The model proposed for describing the NPQ versus E curve is based on the main assumption that NPQ is mostly because of q_E, the "energy-quenching" associated to the buildup of the transthylakoid ΔpH and the operation of the XC. This assumption is generally supported by the finding of strong linear relationships between NPQ and de-epoxidized xanthophylls in all groups investigated (plants, green algae, diatoms, and Chrysophyceae) and under a wide range of experimental conditions.

However, besides q_E, NPQ also quantifies the fluorescence quenching caused by state transitions (q_T) or by photoinhibition (q_I) that may potentially significantly affect the NPQ versus E curves. The q_T is relevant in phycobilisome-containing organisms (cyanobacteria and red algae) (Campbell et al. 1998; Mullineaux and Emlyn-Jones 2005), although not as much in higher plants and green algae (Pfannschmidt 2005; Eberhard et al. 2008; Ruban and Johnson 2009), and it does not occur for the Heterokontophyta (Lavaud 2007). When occurring, q_T is not significant in light conditions triggering q_E-related NPQ (Mullineaux and Emlyn-Jones 2005; Tikkanen et al. 2006; Ruban and Johnson 2009). With the exception of some land plants (overwintering conifers and tropical evergreen species), q_I origin is not clearly defined and it requires particular conditions such as prolonged environmental stress (Müller et al. 2001; Demmig-Adams and Adams 2006; Horton et al. 2008).

The effects of q_T or q_I on the light–response curve of NPQ likely consist of a general change in curve shape, through the increase of NPQ at low-light levels (for q_T) and of NPQ_m (for q_I). However, these components of NPQ may be expected not to significantly affect the NPQ versus E curves measured under the usually applied experimental protocols. This is because the duration of the light steps commonly applied ($\leq$2–3 min, and much shorter in the case of RLCs) corresponds to light doses clearly different than those required to induce both q_T and q_I (Campbell et al. 1998; Müller et al. 2001; Demmig-Adams and Adams 2006; Horton et al. 2008; Ruban and Johnson 2009).

The same reasoning applies to another implicit assumption of the model that during the generation of a light curve q_E is due solely to the development of the ΔpH and the subsequent de-epoxidation of the present (and susceptible of being de-epoxidized) pool of xanthophylls. In fact, it is well established that exposure to high-light can induce the de novo synthesis of XC pigments (e.g., Olaizola and Yamamoto 1994; D'Haese et al. 2004; Lavaud et al. 2004; Demmig-Adams and Adams 2006). This process causes the accumulation of de-epoxidized forms, which could result in the linear increase of NPQ in the high-light part of the curve. Again, the de novo synthesis requires the prolonged exposure to very high irradiances (e.g., Lavaud et al. 2004; Demmig-Adams and Adams 2006; Lavaud 2007), well above the light doses applied during the construction of NPQ light–response curves.

Nevertheless, even if significant q_T, q_I, or de novo pigment synthesis do occur, the resulting curve may still be of the same general shape and describable by the model. In fact, this study showed that the model fits very well to data obtained in a wide range of experimental conditions in which the occurrence of any of these processes cannot be completely ruled out (Table 2). In this case, however, care should be taken in interpreting and comparing the model parameters estimated for different species or condition, as they may be affected differently by processes other than the buildup of the ΔpH and the XC. In the case of organisms with impaired operation of the XC (mutants or inhibitor-treated samples), the model was nevertheless shown to be of value, providing a useful quantitative characterization of the light response of NPQ.

Another major assumption of the model is that the formation of q_E, through the de-epoxidation of Vx or DD generated by the acidification of the lumen relates to incident irradiance following the generic conditions of application of the Hill equation, i.e., that NPQ can be considered as allosterically regulated by irradiance through the buildup of the transthylakoidal ΔpH. This assumption is partially supported by the finding that, in isolated plant chloroplasts, the regulation of q_E is of allosteric nature, resulting in response curves of q_E as a function of ΔpH of sigmoidal shape, shown to be adequately described by the Hill equation (Pfündel and Dilley 1993; Ruban et al. 2001; Takizawa et al. 2007; Pérez-Bueno et al. 2008). This sigmoidicity is attributed to the protonation of binding sites of the LHC protein *Psbs* induced by lumen acidification, and subsequent conformational changes within the LHC, switching the de-epoxidized xanthophylls to an "activated" state. It is taken as an indication of allosteric regulation of q_E, resulting from proton binding showing positive cooperativity, and the "activated" de-epoxidized xanthophylls Zx (Horton et al. 2000; Horton et al. 2008; Li et al. 2009) or DT (Goss et al. 2006; Lavaud and Kroth 2006) acting as a positive effector.

The strong physiological basis of the proposed model is likely to explain its success to cope with a large diversity of light–response curve characteristics. Other mathematical models have also been used to successfully describe NPQ versus E curves, namely, an exponential saturation function, the Michaelis–Menten function, and a hyperbolic tangent function (Ritchie 2008). However, these models have only been tested on a reduced dataset, and on light curves of low sigmoidicity. Interestingly, the model that yielded the better fit to experimental data was the Michaelis–Menten equation (Ritchie 2008), a particular case of the model proposed in this study.

Model fitting to NPQ versus E curves

The usefulness of the model was demonstrated by the possibility to estimate NPQ_m despite the fact that in most cases the curves did not reach a saturation plateau within the range of irradiances applied (e.g., Fig. 1a). When assuming NPQ to represent mostly q_E, the maximum NPQ reached by a sample quantifies its photoprotective potential through the dissipation of excessive light energy.

By applying the model, curves measured under different experimental conditions can be readily compared and changes in NPQ_m (e.g., following changes in growth light conditions) can be quantified, which would be otherwise impossible. The accurate estimation of NPQ_m is also required for quantifying E_{50}, which, in some cases of strict relationship (e.g., for most Heterokontophyta; Lavaud et al. 2004; Lavaud 2007), is interpretable as the light level corresponding to the de-epoxidation and "activation" of the xanthophyll convertible pool necessary to induce half of the maximal NPQ. The size of the xanthophyll convertible pool can be very different in VAZ and DD–DT organisms varying with species and growth conditions, ranging between 50 and 70% (Lavaud 2007; Goss and Jakob 2010). Again, the fit of Eq. 2 to NPQ versus E curves provided an adequate form of characterizing how promptly the XC is ΔpH-activated when responding to an increase in incident irradiance.

However, although NPQ_m and E_{50} can be grossly estimated by visual inspection of the curves (at least when saturation is reached for the light levels applied), the curve sigmoidicity can hardly be characterized quantitatively without the fit of the model and estimation of n. The sigmoidicity coefficient was found to vary around 1.5–2.0, values corresponding to positive cooperativity and thus indicating the allosteric regulation of NPQ by light. Minimum n values averaged about 1 (reaching significantly lower values only for cases of XC impairment), indicating that negative cooperativity is not involved in the regulation of processes underlying NPQ. These results generally support that the allosteric nature known for the more fundamental regulation of q_E by ΔpH in plants (Ruban et al. 2001; Li et al. 2009) holds for the relationship of NPQ to irradiance in a large diversity of photosynthetic organisms.

The Hill coefficient has been interpreted as representing the number of allosteric regulators (D'Haese et al. 2004). Considering the diversity of factors likely to contribute to the NPQ versus E curve (Demmig-Adams and Adams 2006; Eberhard et al. 2008; Horton et al. 2008; Li et al. 2009), some of them not fully identified in some photosynthetic taxa (Lavaud 2007), n should be considered simply as an empirical coefficient informing on the degree of allostery and serving as a practical descriptor of the curve shape.

Relationship of NPQ light response to photoacclimation status

The modelling of the NPQ versus E curves opens the new possibility of quantitatively comparing the light responses of NPQ and of photochemistry or ETR. Photosynthesis and ETR light–response curves are very commonly used as a form of characterizing the photoacclimation status of photosynthetic organisms, through the estimation of the parameters of a number of available models (Henley 1993; Behrenfeld et al. 2004; Ralph and Gademann 2005; Guarini and Moritz 2009; Perkins et al. 2010). By describing the NPQ versus E curve by a small set of meaningful parameters, the light response of NPQ can be characterized relatively to the one of ETR or photosynthetic rate.

This possibility is useful for the definition of the light levels corresponding to the onset of NPQ (e.g., activation of the XC) relatively to the saturation of photochemistry. As the light response of NPQ may depend greatly on the photoacclimation status, the characterization and comparison of NPQ versus E curves should be preferably normalized to parameters indicative of photochemistry saturation. Furthermore, the comparison of the NPQ and ETR light responses is also of interest because it provides insight on the way an organism combines the responses of photochemistry and of photoprotective processes to changes in ambient light. However, without adequate parameterization of the NPQ light–response, this question can be answered only approximately.

Despite its simplicity, the indices E_{50}/E_k and NPQ_{E_k} here proposed provide an efficient form of comparing the light levels for which NPQ reaches significant values and photochemistry reaches saturation. The application of these indices allowed quantifying the delay of the light response of NPQ relatively to the saturation of photochemistry. Under the assumption that NPQ mostly represents q_E, it showed that it takes about three times the irradiance at E_k for half of q_E to develop and that, at E_k, the formation of q_E is still at relatively low levels, providing typically less than one fifth of maximum photoprotective capacity. For the cases when q_E is strictly related to the XC operation (e.g., in most of Heterokontophyta; Lavaud et al. 2004; Lavaud 2007), the values of the indices E_{50}/E_k and NPQ_{E_k} can be interpreted in terms of the de-epoxidation state of the convertible pool of xanthophylls and their "activation" on LHC protonation. Yet the modelling of the NPQ versus E curve may allow for the development of other indices that better characterize this relationship.

Interestingly, the meta-analysis carried out in this study showed consistent differences between the relationships of NPQ light response to photoacclimation status in organisms with VAZ and DD–DT types of XC. The fact that these differences were found despite the diversity in taxa and growth conditions may indicate that they are because of fundamental differences in the way the two types of organisms cope with high light, especially regarding the underlying q_E mechanism and regulation of the XC, illustrating the advantages provided by the quantitative description of the NPQ versus E curve.

Acknowledgments We thank Glória Pinto, Eleazar Rodriguez, and Armando Costa for helping with the seeding of the *Arabidopsis* plants. This study was supported by FCT—Fundação para a Ciência e a Tecnologia, grant SFRH/BSAB/962/2009 to J. Serôdio, by the French consortium CPER-Littoral to J. Lavaud, and by the CNRS—Centre National de la Recherche Scientifique (programme 'chercheurs invités') to both. We thank two anonymous reviewers for critical comments on the manuscript.

References

Bailleul B, Rogato A, Martino A, Coesel S, Cardol P, Bowler C, Falciatore A, Finazzi G (2010) An atypical member of the light-harvesting complex stress-related protein family modulates diatom responses to light. Proc Natl Acad Sci USA 107: 18214–18219

Baker NR, Oxborough K (2004) Chlorophyll fluorescence as probe of plant photosynthetic productivity. In: Papageorgiou GC, Govindjee (eds) Chlorophyll *a* fluorescence: a signature of photosynthesis. Springer, Dordrecht, pp 65–82

Behrenfeld MJ, Prasil O, Babin M, Bruyant F (2004) In search of a physiological basis for covariations in light-limited and light-saturated photosynthesis. J Phycol 40:4–25

Bilger W, Bjorkman O (1990) Role of the xanthophyll cycle in photoprotection elucidated by measurements of light-induced absorbance changes, fluorescence and photosynthesis in leaves of *Hedera canariensis*. Photosynth Res 25:173–185

Burritt DJ, Mackenzie S (2003) Antioxidant metabolism during acclimation of *Begonia* × *erytrophylla* to high light levels. Ann Bot 91:783–794

Campbell D, Hurry V, Clarke AK, Gustafsson P, Gunnar Ö (1998) Chlorophyll fluorescence analysis of cyanobacterial photosynthesis and acclimation. Microbiol Molec Biol Rev 62:667–683

Cosgrove J, Borowitzka M (2006) Applying pulse amplitude modulation (PAM) fluorometry to microalgae suspensions: stirring potentially impacts fluorescence. Photosynth Res 88:343–350

Cruz S, Serôdio J (2008) Relationship of rapid light curves of variable fluorescence to photoacclimation and non-photochemical quenching in a benthic diatom. Aquat Bot 88:256–264

D'Haese D, Vandermeiren K, Caubergs RJ, Guisez Y, De Temmerman L, Horemans N (2004) Non-photochemical quenching kinetics during the dark to light transition in relation to the formation of antheraxanthin and zeaxanthin. J Theor Biol 227:175–186

Demmig-Adams B, Adams WW (2006) Photoprotection in an ecological context: the remarkable complexity of thermal energy dissipation. New Phytol 172:11–21

Dimier C, Corato F, Saviello G, Brunet C (2007a) Photophysiological properties of the marine picoeukaryote *Picochlorum* Rcc 237 (Trebouxiophyceae, Chlorophyta). J Phycol 43:275–283

Dimier C, Corato F, Tramontano F, Brunet C (2007b) Photoprotection and xanthophyll-cycle activity in three marine diatoms. J Phycol 43:937–947

Eberhard S, Finazzi G, Wollman F (2008) The dynamics of photosynthesis. Ann Rev Gen 42:463–515

Eilers PH, Peeters JC (1988) A model for the relationship between light intensity and the rate of photosynthesis in phytoplankton. Ecol Model 42:199–215

Elrad D, Niyogi KK, Grossman AR (2002) A major light-harvesting polypeptide of photosystem II functions in thermal dissipation. Plant Cell 14:1801–1816

Geel C, Verluis W, Snel JF (1997) Estimation of oxygen evolution by marine phytoplankton from measurement of the efficiency of photosystem II electron flow. Photosynth Res 51:61–70

Genty B, Briantais JM, Baker NR (1989) The relationship between the quantum yield of photosynthetic electron transport and quenching of chlorophyll fluorescence. Biochim Biophys Acta 990:87–92

Goss R, Jakob T (2010) Regulation and function of xanthophyll cycle-dependent photoprotection in algae. Photosynth Res 106:103–122

Goss R, Pinto EA, Wilhelm C, Richter M (2006) The importance of a highly active and ΔpH-regulated diatoxanthin epoxidase for the regulation of the PS II antenna function in diadinoxanthin cycle containing algae. J Plant Physiol 163:1008–1021

Guarini J, Moritz C (2009) Modelling the dynamics of the electron transport rate measured by PAM fluorimetry during rapid light curve experiments. Photosynthetica 47:206–214

Guillard RRL, Ryther JH (1962) Studies of marine phytoplanktonic diatoms. I. *Cyclotella nana* Hustedt and *Detonula confervaceae* (Cleve) Gran. Can J Microbiol 8:229–239

Havaux M, Kloppstech K (2001) The protective functions of carotenoid and flavonoid pigments against excess visible radiation at chilling temperature investigated in *Arabidopsis npq* and *tt* mutants. Planta 213:953–966

Henley WJ (1993) Measurement and interpretation of photosynthetic light–response curves in algae in the context of photoinhibition and diel changes. J Phycol 29:729–739

Herlory O, Richard P, Blanchard GF (2007) Methodology of light response curves: application of chlorophyll fluorescence to microphytobenthic biofilms. Mar Biol 153:91–101

Horton P, Ruban AV, Wentworth M (2000) Allosteric regulation of the light-harvesting system of photosystem II. Philos Trans Royal Soc London Series B 355:1361–1370

Horton P, Johnson MP, Perez-Bueno ML, Kiss AZ, Ruban AV (2008) Photosynthetic acclimation: does the dynamic structure and macro-organisation of photosystem II in higher plant grana membranes regulate light harvesting states? FEBS J 275:1069–1079

Jakob T, Goss R, Wilhelm C (1999) Activation of diadinoxanthin de-epoxidase due to a chlororespiratory proton gradient in the dark in the diatom *Phaeodactylum tricornutum*. Plant Biol 1:76–82

Johnson ML (2008) Nonlinear least-squares fitting methods. In: Correia J, Detrich H (eds) Methods in cell biology, vol 84. Elsevier Academic Press, San Diego, pp 781–805

Jung H-S, Niyogi KK (2009) Quantitative genetic analysis of thermal dissipation in Arabidopsis. Plant Physiol 150:977–986

Kromkamp JC, Dijkman NA, Peene J, Simis SGH, Gons HJ (2008) Estimating phytoplankton primary production in Lake IJsselmeer (The Netherlands) using variable fluorescence (PAM-FRRF) and C-uptake techniques. Eur J Phycol 43:327–344

Kropuenske LR, Mills MM, Dijken GL, Bailey S, Robinson DH, Welschmeyer NA, Arrigo KR (2009) Photophysiology in two major Southern Ocean phytoplankton taxa: photoprotection in *Phaeocystis antarctica* and *Fragilariopsis cylindrus*. Limnol Oceanogr 54:1176–1196

Krupenina NA, Bulychev AA (2007) Action potential in a plant cell lowers the light requirement for non-photochemical energy-dependent quenching of chlorophyll fluorescence. Biochim Biophys Acta 1767:781–788

Lavaud J (2007) Fast regulation of photosynthesis in diatoms: mechanisms, evolution and ecophysiology. Funct Plant Sci Biotechnol 1:267–287

Lavaud J, Kroth PG (2006) In diatoms, the transthylakoid proton gradient regulates the photoprotective non-photochemical fluorescence quenching beyond its control on the xanthophyll cycle. Plant Cell Physiol 47:1010–1016

Lavaud J, Rousseau B, Gorkom HJ, Etienne A (2002) Influence of the diadinoxanthin pool size on photoprotection in the marine planktonic diatom. Plant Physiol 129:1398–1406

Lavaud J, Rousseau B, Etienne AL (2004) General features of photoprotection by energy dissipation in planktonic diatoms (Bacillariophyceae). J Phycol 40:130–137

Lavaud J, Strzepek RF, Kroth PG (2007) Photoprotection capacity differs among diatoms: possible consequences on the spatial distribution of diatoms related to fluctuations in the underwater light climate. Limnol Oceanogr 52:1188–1194

Li X-P, Björkman O, Shih C, Grossman AR, Rosenquist M, Jansson S, Niyogi KK (2000) A pigment-binding protein essential for regulation of photosynthetic light harvesting. Nature 403: 391–395

Li Z, Wakao S, Fischer BB, Niyogi KK (2009) Sensing and responding to excess light. Annu Rev Plant Biol 60:239–260

Lokstein H, Tian L, Polle JE, DellaPenna D (2002) Xanthophyll biosynthetic mutants of *Arabidopsis thaliana*: altered nonphotochemical quenching of chlorophyll fluorescence is due to changes in photosystem II antenna size and stability. Biochim Biophys Acta 1553:309–319

Marschall M, Proctor MCF (2004) Are bryophytes shade plants? Photosynthetic light responses and proportions of chlorophyll *a*, chlorophyll *b* and total carotenoids. Ann Bot 94:593–603

Mouget J-L, Tremblin G (2002) Suitability of the fluorescence monitoring system (FMS, Hansatech) for measurement of photosynthetic characteristics in algae. Aquat Bot 74:219–231

Müller P, Li X-P, Niyogi KK (2001) Non-photochemical quenching. A response to excess light energy. Plant Physiol 125:1558–1566

Müller-Moulé P, Conklin PL, Niyogi KK (2002) Ascorbate deficiency can limit violaxanthin de-epoxidase activity in vivo. Plant Physiol 128:970–977

Müller-Moulé P, Golan T, Niyogi KK (2004) Ascorbate-deficient mutants of Arabidopsis grow in high light despite chronic photooxidative stress. Plant Physiol 134:1163–1172

Mullineaux CW, Emlyn-Jones D (2005) State transitions: an example of acclimation to low-light stress. J Exp Bot 56:389–393

Munekage Y, Hojo M, Meurer J, Endo T, Tasaka M, Shikanai T (2002) *PGR5* is involved in cyclic electron flow around photosystem I and is essential for photoprotection in *Arabidopsis*. Cell 110:361–371

Munshi MK, Kobayashi Y, Shikanai T (2006) Chlororespiratory reduction 6 is a novel factor required for accumulation of the chloroplast NAD(P)H dehydrogenase complex in *Arabidopsis*. Plant Physiol 141:737–744

Niyogi KK, Grossman AR, Björkman O (1998) *Arabidopsis* mutants define a central role for the xanthophyll cycle in the regulation of photosynthetic energy conversion. Plant Cell 10:1121–1134

Olaizola M, Yamamoto HY (1994) Short-term response of the diadinoxanthin cycle and fluorescence yield to high irradiance in *Chaetoceros muelleri* (Bacillariophyceae). J Phycol 30:606–612

Ort DR (2001) When there is too much light. Plant Physiol 125:29–32

Osmond B, Badger M, Maxwell K, Björkman O, Leegood R (1997) Too many photons: photorespiration, photoinhibition and photooxidation. Trends Plant Sci 2:119–121

Peers G, Truong TB, Ostendor E, Busch A, Elrad D, Grossman AR, Hippler M, Niyogi KK (2009) An ancient light-harvesting protein is critical for the regulation of algal photosynthesis. Nature 462:518–522

Pérez-Bueno ML, Johnson MP, Zia A, Ruban AV, Horton P (2008) The Lhcb protein and xanthophyll composition of the light harvesting antenna controls the ΔpH-dependency of non-photochemical quenching in *Arabidopsis thaliana*. FEBS Lett 582:1477–1482

Perkins RG, Mouget J-L, Lefebvre S, Lavaud J (2006) Light response curve methodology and possible implications in the application of chlorophyll fluorescence to benthic diatoms. Mar Biol 149:703–712

Perkins RG, Kromkamp J, Serôdio J, Lavaud J, Jesus B, Mouget J-L, Forster R, Lefebvre S (2010) The application of variable chlorophyll fluorescence to microphytobenthic biofilms. In: Suggett D, Prasil O, Borowitza MA (eds) Chlorophyll *a* fluorescence in aquatic sciences: methods and applications. Developments in applied phycology, 4th edn. Springer, Dordrecht, pp 273–275

Pfannschmidt T (2005) Acclimation to varying light qualities: toward the functional relationship of state transitions and adjustment of photosystem stoichiometry. J Phycol 41:723–725

Pfündel EE, Dilley RA (1993) The pH dependence of violaxanthin deepoxidation in isolated pea chloroplasts. Plant Physiol 101:65–71

Press WH, Teukolsky S, Vetterling W, Flannery B (1996) Numerical recipes in Fortran 90. The art of parallel scientific computing, 2nd edn. Cambridge University Press, Cambridge

Ralph PJ, Gademann R (2005) Rapid light curves: a powerful tool to assess photosynthetic activity. Aquat Bot 82:222–237

Ralph PJ, Gademann R, Larkum AW (2001) Zooxanthellae expelled from bleached corals at 33°C are photosynthetically competent. Mar Ecol Prog Ser 220:163–168

Ritchie RJ (2008) Fitting light saturation curves measured using modulated fluorometry. Photosynth Res 96:201–215

Rodríguez-Calcerrada J, Pardos JA, Gil L, Aranda I (2007) Acclimation to light in seedlings of *Quercus petraea* (Mattuschka) Liebl. and *Quercus pyrenaica* Willd. planted along a forest-edge gradient. Trees 21:45–54

Ruban AV, Johnson MP (2009) Dynamics of higher plant photosystem cross-section associated with state transitions. Photosynth Res 99:173–183

Ruban AV, Wentworth M, Horton P (2001) Kinetic analysis of nonphotochemical quenching of chlorophyll fluorescence. 1. Isolated chloroplasts. Biochemistry 40:9896–9901

Serôdio J, Vieira S, Cruz S, Coelho H (2006) Rapid light–response curves of chlorophyll fluorescence in microalgae: relationship to steady-state light curves and non-photochemical quenching in benthic diatom-dominated assemblages. Photosynth Res 90:29–43

Takizawa K, Cruz JA, Kanazawa A, Kramer DM (2007) The thylakoid proton motive force in vivo. Quantitative, noninvasive probes, energetics, and regulatory consequences of light-induced *pmf*. Biochim Biophys Acta 1767:1233–1244

Tellinghuisen J (2008) Stupid statistics!. In: Correia J, Detrich H (eds) Methods in cell biology, vol 84. Elsevier Academic Press, San Diego, pp 739–780

Tikkanen M, Pippo M, Suorsa M, Sirpio S, Mulo P, Vainonen J, Vener A, Allahverdiyeva Y, Aro EM (2006) State transitions revisited: a buffering system for dynamic low light acclimation of *Arabidopsis*. Plant Molec Biol 62:779–793

Voet D, Voet JG (1990) Biochemistry. John Wiley and Sons, New York